

Proton Transfer Reactions and Ion-Molecule Reactions of Ionized XCH_2CH_2Y (X and Y = OH or NH_2)

Sung-Seen Choi* and Hun-Young So†

Department of Applied Chemistry, Sejong University, Seoul 143-747, Korea. *E-mail: sschoi@sejong.ac.kr

†Korea Research Institute of Standards and Science, P.O. Box 102, Yuseong, Daejeon 305-600, Korea

Received October 25, 2005

Proton transfer reactions and ion-molecule reactions of bifunctional ethanes of $H_2NCH_2CH_2NH_2$, $H_2NCH_2CH_2OH$, and $HOCH_2CH_2OH$ were studied using Fourier transform mass spectrometry (FTMS). The rate constants for proton transfer reactions between the fragment ions and neutral molecules were obtained from the temporal variation of the ion abundances. The rate constants were consistent with the heats of reaction. The fastest proton transfer reactions were the reactions of CH_2N^+ , CHO^+ , and CH_3O^+ for $H_2NCH_2CH_2NH_2$, $H_2NCH_2CH_2OH$, and $HOCH_2CH_2OH$, respectively. The $[M+13]^+$ ion was formed by the ion-molecule reaction between $H_2C=NH_2^+$ or $H_2C=OH^+$ and the neutral molecule. The major product ions generated from the ion-molecule reactions between the protonated molecule and neutral molecule were $[2M+H]^+$, $[M+27]^+$, and $[M+15]^+$.

Key Words : Proton transfer reaction, Ion-molecule reaction, Ethylenediamine, Ethanolamine, Ethylene glycol

Introduction

As a fundamental understanding of mass peaks observed in a mass spectrum, structures of ions and mechanistic and dynamic details of fragmentation processes have been subject of various compounds and mass analyzers.¹⁻⁴ The fragmentation patterns of a molecule under a specific ionization method depend upon energy deposited in ionization process, pressure of environment where ion resides, and time given to facilitate ion-molecule reaction. Fourier transform ion cyclotron resonance (FT/ICR) mass spectrometry has been widely used in the study of gas phase chemistry.⁵⁻⁹ Its capability of trapping ions and high resolution has motivated researchers to utilize Fourier transform mass spectrometry (FTMS) as one of the premier methods for exploring gas phase ion-molecule chemistry.

Molecules with specific functional group undergo typical fragmentation patterns, which can be used to obtain structural information. Ionized alcohols are fragmented and rearranged as water molecules are lost.¹⁰⁻¹² Blanc and coworkers¹³ reported that a five-membered ring involving oxygen was formed by loss of water molecule from $HO(CH_2)_4OH^+$. Burgers and coworkers¹⁴ studied thermodynamically stable isomers of ionized ethylene glycol by experiments and high-level molecular orbital theoretical calculations. Major fragment ions of ionized ethylenediamine and ethanolamine are $[M-H]^+$, m/z 44, and m/z 30 ions.¹⁵ Audier and coworkers¹⁶ studied the formation of cyclic diols by chemically ionizing a bifunctional organic molecule, $HO(CH_2)_4NH_2$, and proposed that the protonated tetrahydrofuran is formed from $HO(CH_2)_4NH_3^+$ by loss of NH_3 while the protonated pyrrolidine is formed from $H_2N(CH_2)_4OH_2^+$ by loss of H_2O .

In the ICR cell, product ions in the cell can react with

neutral molecules (ion-molecule reactions).^{7,9} In general, a predominant product ion formed from proton transfer reactions between fragment ions and neutral molecules is protonated molecule, $[M+H]^+$. In the present work, we investigated proton transfer reactions and ion-molecule reactions of ionized ethanolamine, ethylenediamine, and ethylene glycol by varying the ion trapping time. Proton transfer reactions between the fragment ions and neutral molecules were investigated and their rate constants were obtained. The formations of ions with an m/z value larger than a molecular ion were explained by ion-molecule reactions. The plausible structures of observed ions were also investigated by theoretical calculations.

Experimental Section

All the experiments were carried out on an Extrel FTMS 2000 Fourier transform ion cyclotron resonance (FT/ICR) mass spectrometer. The instrument is equipped with two diffusion pumps attached to dual ion trapping cells aligned collinearly in a superconducting magnet of 3.1 Tesla. The nominal value of background pressure measured with nude ion gauge was lower than 1×10^{-8} Torr. Samples were introduced into the cell through a leak valve. The electron impact energy was 70 eV. The sample pressure was about 10^{-6} Torr and the ion trapping time was varied in range of $1.0-1.0 \times 10^4$ ms.

Ethylenediamine, ethanolamine, and ethylene glycol obtained from Aldrich Co. were used without further purification. The heats of formation of ions, which were not available from literature,¹⁷ were calculated by the AM1 semiempirical method¹⁸ to investigate the stabilities of observed ions. The calculation results were used to elucidate the heats of reaction to understand the proton transfer reactions and ion-molecule reactions.

Results and Discussion

The electron ionization mass spectra of ethylenediamine ($\text{H}_2\text{NCH}_2\text{CH}_2\text{NH}_2$, **DA**), ethanolamine ($\text{H}_2\text{NCH}_2\text{CH}_2\text{OH}$, **EA**), and ethylene glycol ($\text{HOCH}_2\text{CH}_2\text{OH}$, **EG**) at 70 eV of electron ionization energy are shown in Figures 1-4. At the short ion trapping time of 1.0 ms, the most abundant fragment ions are m/z 30 ($\text{H}_2\text{C}=\text{NH}_2^+$) for **DA** and **EA**, and m/z 31 ($\text{H}_2\text{C}=\text{OH}^+$) for **EG** as shown in Figure 1. At the longer ion trapping time, product ions having larger mass than the molecular ion become the most abundant ions as shown in Figures 2-4.

Proton Transfer Reactions. Relative abundances of the fragment ions are, on the whole, decreased by increasing the ion trapping time, while the protonated molecules, $[\text{M}+\text{H}]^+$, are increased. Variations of the major fragment ions, molecular ion, and $[\text{M}+\text{H}]^+$ with the ion trapping time were plotted (Figures 5-7). The fragment ions are linearly decreased with increase of the ion trapping time after 30, 50, and 60 ms for **DA**, **EA**, and **EG**, respectively, while the $[\text{M}+\text{H}]^+$ becomes the most abundant ion. This is due to the proton transfer reactions between the fragment ions and neutral molecules. The rate constants for the proton transfer reactions of $\text{FH}^+ + \text{M} \rightarrow [\text{M}+\text{H}]^+ + \text{F}$, where FH^+ denotes the fragment ion, were obtained from the experimental results in Figures 5-7.

Rate constants for the proton transfer reactions were calculated after 30, 50, and 60 ms of the ion trapping times

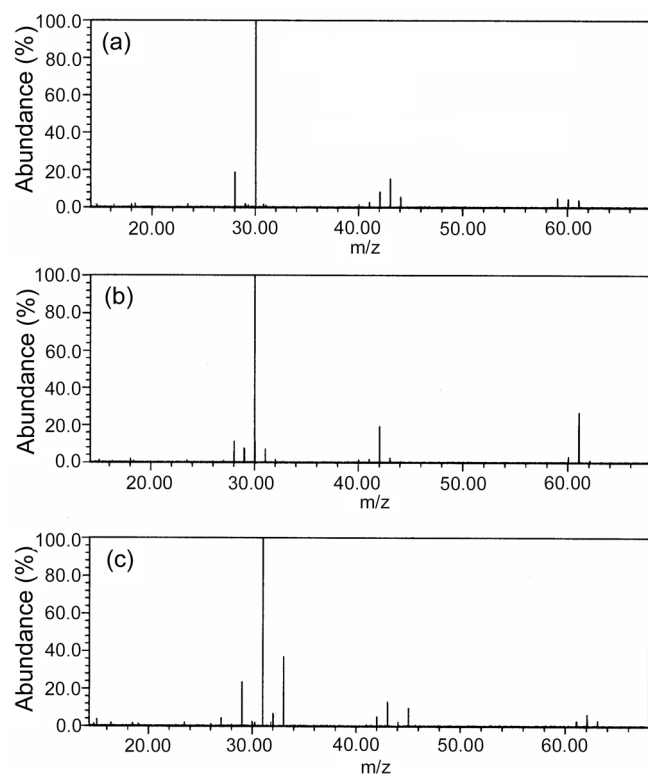


Figure 1. Electron ionization mass spectra of ethylenediamine (a), ethanolamine (b), and ethylene glycol (c) at the electron ionization energy of 70 eV and the ion trapping time of 1 ms. The pressures are about 3.0×10^{-6} Torr.

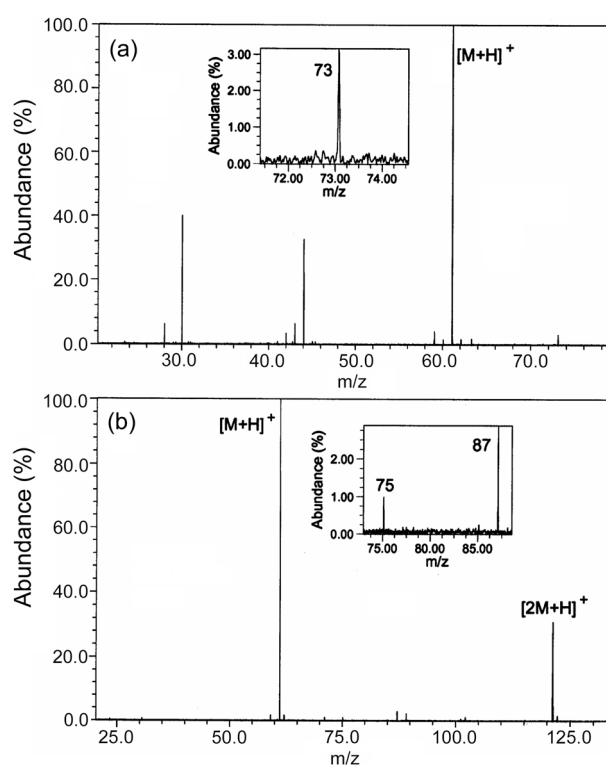


Figure 2. Electron ionization mass spectra of ethylenediamine at 70 eV of the electron ionization energy. The sample pressures and ion trapping times are 3.0×10^{-6} Torr and 50 ms (a) 4.0×10^{-6} Torr and 10 s (b).

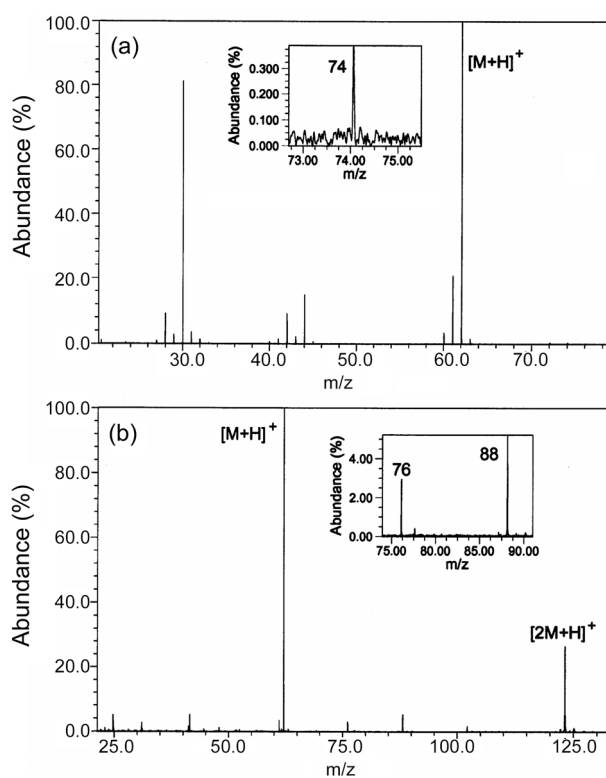


Figure 3. Electron ionization mass spectra of ethanolamine at 70 eV of the electron ionization energy. The sample pressures and ion trapping times are 3.0×10^{-6} Torr and 50 ms (a) 4.0×10^{-6} Torr and 10 s (b).

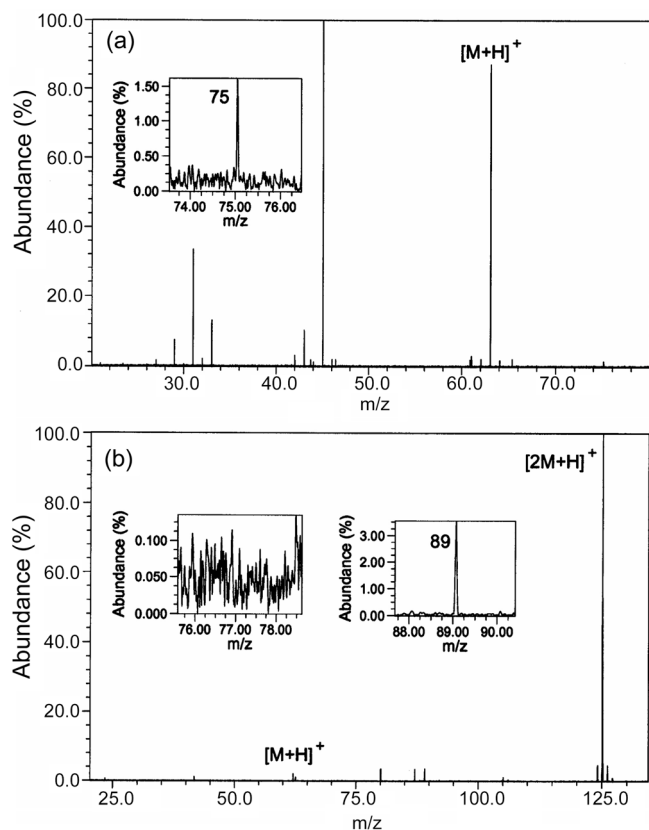


Figure 4. Electron ionization mass spectra of ethylene glycol at 70 eV of the electron ionization energy. The sample pressures and ion trapping times are 3.0×10^{-6} Torr and 50 ms (a) 4.0×10^{-6} Torr and 10 s (b).

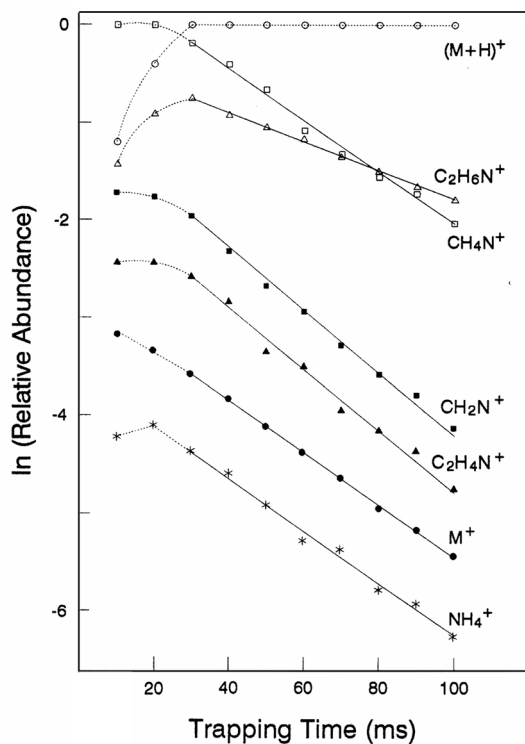


Figure 5. Temporal variation of the ion abundances of ethylenediamine. The electron ionization energy of 70 eV and the sample pressure is about 3.0×10^{-6} Torr.

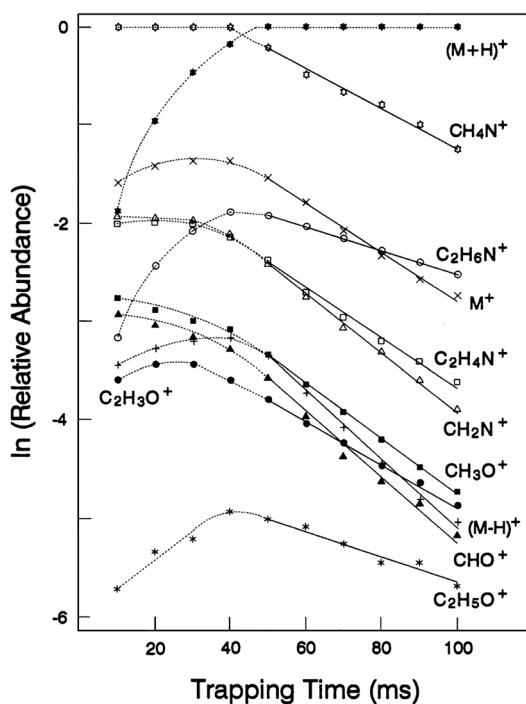


Figure 6. Temporal variation of the ion abundances of ethanolamine. The electron ionization energy of 70 eV and the sample pressure is about 3.0×10^{-6} Torr.

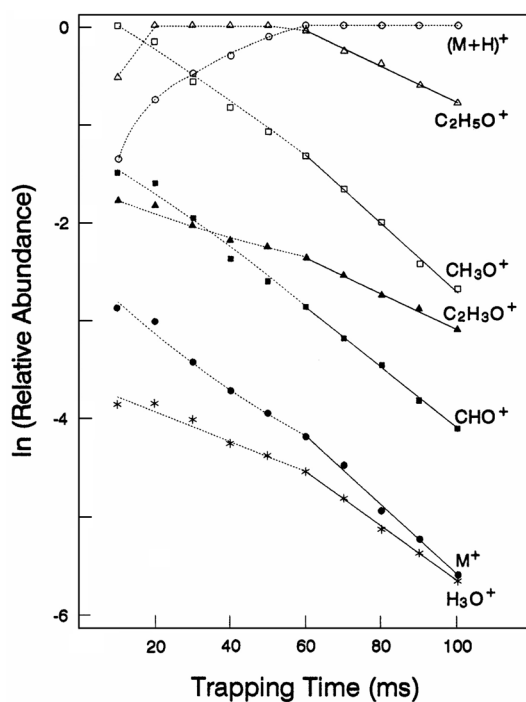


Figure 7. Temporal variation of the ion abundances of ethylene glycol. The electron ionization energy of 70 eV and the sample pressure is about 3.0×10^{-6} Torr.

for DA, EA, and EG, respectively. Relative ion abundances of the fragment ions were calculated by comparing the most abundant ion, $[M+H]^+$. Let the relative ion abundance of the $[M+H]^+$ be 1.00. The relative ion abundances of the FH^+ s decrease linearly. Since the relative ion abundances of NH_4^+

Table 1. Rate constants for the proton transfer reactions, $\text{FH}^+ + \text{M} \rightarrow \text{F} + [\text{M}+\text{H}]^+$ *

Fragment ion	$k (\times 10^{-10} \text{ cm}^3 \cdot \text{molecule}^{-1} \cdot \text{s}^{-1})$		
	$\text{H}_2\text{NCH}_2\text{CH}_2\text{NH}_2$	$\text{HOCH}_2\text{CH}_2\text{NH}_2$	$\text{HOCH}_2\text{CH}_2\text{OH}$
Molecular ion	2.67	3.22	3.65
$\text{C}_2\text{H}_6\text{N}^+$	1.58	1.56	–
$\text{C}_2\text{H}_4\text{N}^+$	3.27	3.43	–
CH_4N^+	2.58	2.70	–
CH_2N^+	3.33	3.84	–
NH_4^+	2.75	3.12	–
$\text{C}_2\text{H}_5\text{O}^+$	–	1.66	1.88
$\text{C}_2\text{H}_3\text{O}^+$	–	2.91	1.82
CH_3O^+	–	3.53	3.65
CHO^+	–	4.26	3.23
H_3O^+	–	3.74	3.02

*Rate constants were calculated from Figures 5-7.

and H_3O^+ for **EA** were too small (less than 0.003), the temporal variations for NH_4^+ and H_3O^+ were not plotted in Figure 6. The proton transfer reactions of **EA** are faster than or almost equal to those of **DA** and **EG** as listed in Table 1. This tendency is well consistent with the heats of reaction for the proton transfer reactions as shown in Table 2. The heats of reaction for the proton transfer reactions of **EA** are lower than those of **DA** and **EG**. All the proton transfer reactions between the fragment ions and neutral molecules are exothermic.

For **DA** and **EA**, the rate constants of the fragment ions containing a nitrogen atom are consistent with the calculated heats of reaction. When the proton transfer reaction is more exothermic, it becomes faster. Among the proton transfer reactions of the fragment ions containing a nitrogen atom, the fastest one is the reaction of $\text{HC}\equiv\text{NH}^+$ while the slowest one is that of $\text{C}_2\text{H}_6\text{N}^+$. The rate constants of the fragment ions containing an oxygen atom of **EA** are relatively consistent with the heats of reaction. However, the rate constants of $\text{C}_2\text{H}_5\text{O}^+$ and $\text{C}_2\text{H}_3\text{O}^+$ are not consistent with the heats of reaction. This disagreement suggests that there are

two or more possible structures of $\text{C}_2\text{H}_3\text{O}^+$. The $\text{C}_2\text{H}_3\text{O}^+$ can have a cyclic or linear structure. The cyclic $\text{CH}_2\text{CH}=\text{O}^+$ ($\Delta H_f = 1226 \text{ kJ/mol}$)¹⁹ is less stable than the linear $\text{CH}_3\text{C}\equiv\text{O}^+$ ($\Delta H_f = 657 \text{ kJ/mol}$). The heat of reaction for the proton transfer reaction of the cyclic $\text{CH}_2\text{CH}=\text{O}^+$ will be much lower than that of the linear structure when the neutral form is the same. The exact heat of reaction for the proton transfer reaction of the cyclic $\text{CH}_2\text{CH}=\text{O}^+$ of **EA** can not be determined because of the unclearness of the structure of counter neutral molecule. Thus, both the cyclic $\text{CH}_2\text{CH}=\text{O}^+$ and linear $\text{CH}_3\text{C}\equiv\text{O}^+$ are considered as structures of $\text{C}_2\text{H}_3\text{O}^+$.

Ion-Molecule Reactions between $\text{H}_2\text{C}=\text{NH}_2^+$ or $\text{H}_2\text{C}=\text{OH}^+$ and Neutral Molecule. Product ions with m/z larger than the molecular ion are generated by ion-molecule reactions between the fragment ions (or other product ions) and neutral molecules. Mass spectra in Figures 2-4 show the product ions with m/z larger than the molecular ion such as $[\text{M}+\text{H}]^+$, $[\text{M}+13]^+$, $[\text{M}+15]^+$, $[\text{M}+27]^+$, and $[2\text{M}+\text{H}]^+$.

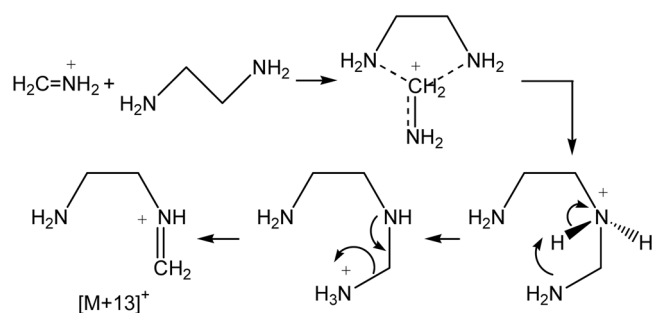
The most abundant fragment ion, $\text{H}_2\text{C}=\text{NH}_2^+$ or $\text{H}_2\text{C}=\text{OH}^+$, can react with a neutral molecule in the ICR cell to generate the product ions with m/z larger than the molecular ion. There are two paths for the ion-molecule reactions between $\text{H}_2\text{C}=\text{NH}_2^+$ or $\text{H}_2\text{C}=\text{OH}^+$ and neutral molecules. The first one is the proton transfer reaction discussed above, which was exothermic. The $[\text{M}+\text{H}]^+$ peaks (m/z 61, 62, and 63 for **DA**, **EA**, and **EG**, respectively) were observed through the long ranges of the ion trapping time. Figures 2-4 show the $[\text{M}+\text{H}]^+$ peaks at 50 ms and 10 s of the ion trapping time. The second one is the formation of $[\text{M}+13]^+$ by loss of NH_3 or H_2O from the ion complex of a neutral molecule and $\text{H}_2\text{C}=\text{NH}_2^+$ or $\text{H}_2\text{C}=\text{OH}^+$.

The $\text{H}_2\text{C}=\text{NH}_2^+$ reacts with a neutral **DA** to form an ion complex of $[\text{H}_2\text{NCH}_2\text{CH}_2\text{NH}_2 \cdots \text{H}_2\text{C}=\text{NH}_2]^+$ as shown in Scheme 1. The complex is rearranged to $\text{H}_2\text{NCH}_2\text{CH}_2\text{NH}-\text{CH}_2\text{NH}_3^+$, and $\text{H}_2\text{NCH}_2\text{CH}_2\text{NH}=\text{CH}_2^+$ is formed by loss of NH_3 . The formations of $[\text{M}+13]^+$ are exothermic except that of $\text{H}_2\text{NCH}_2\text{CH}_2\text{O}=\text{CH}_2^+$ formed from the ion complex of $\text{H}_2\text{C}=\text{NH}_2^+$ and **EA** as listed in Table 3. The $[\text{M}+13]^+$ ions (m/z 73, 74, and 75 for **DA**, **EA**, and **EG**, respectively) were

Table 2. Heats of reaction for the proton transfer reactions, $\text{FH}^+ + \text{M} \rightarrow \text{F} + [\text{M}+\text{H}]^+$. Values in parentheses are heats of formation in kJ/mol *

Fragment ion (ΔH_f)	Neutral molecule (ΔH_f)	ΔH (kJ/mol)		
		$\text{H}_2\text{NCH}_2\text{CH}_2\text{NH}_2$	$\text{HOCH}_2\text{CH}_2\text{NH}_2$	$\text{HOCH}_2\text{CH}_2\text{OH}$
cyclic $\text{CH}_2\text{CH}_2\text{NH}_2^+$ (755)	cyclic $\text{CH}_2\text{CH}_2\text{NH}$ (127)	-40	-48	–
$\text{CH}_3\text{C}\equiv\text{NH}^+$ (835)	$\text{CH}_3\text{C}\equiv\text{N}$ (74)	-173	-181	–
$\text{H}_2\text{C}=\text{NH}_2^+$ (745)	$\text{H}_2\text{C}=\text{NH}$ (78)	-79	-87	–
$\text{HC}\equiv\text{NH}^+$ (955)	$\text{HC}\equiv\text{N}$ (135)	-232	-240	–
NH_4^+ (630)	NH_3 (-46)	-88	-96	–
cyclic $\text{CH}_2\text{CH}_2\text{OH}^+$ (691)	cyclic $\text{CH}_2\text{CH}_2\text{O}$ (-53)	–	-164	-47
$\text{CH}_3\text{C}\equiv\text{O}^+$ (657)	$\text{H}_2\text{C}=\text{C}=\text{O}$ (-48)	–	-125	-8
$\text{H}_2\text{C}=\text{OH}^+$ (703)	$\text{H}_2\text{C}=\text{O}$ (-109)	–	-232	-115
$\text{HC}=\text{O}^+$ (828)	$\text{C}=\text{O}$ (-111)	–	-359	-242
H_3O^+ (591)	H_2O (-242)	–	-253	-136

*Heats of formation for the neutral molecules were obtained from reference 17. Heats of formation for $\text{H}_2\text{NCH}_2\text{CH}_2\text{NH}_2$, $\text{HOCH}_2\text{CH}_2\text{NH}_2$, and $\text{HOCH}_2\text{CH}_2\text{OH}$ are -18, -202, and -389 kJ/mol , respectively, while those for $\text{H}_2\text{NCH}_2\text{CH}_2\text{NH}_3^+$, $\text{HOCH}_2\text{CH}_2\text{NH}_3^+$, and $\text{HOCH}_2\text{CH}_2\text{OH}_2^+$ are 570, 378, and 308 kJ/mol , respectively.



Scheme 1. Formation of $[M+13]^+$ by ion-molecule reaction.

Table 3. Heats of reaction for the ion-molecule reactions of $H_2C=NH_2^+$ or $H_2C=OH^+$ with a neutral molecule. Values in parentheses are heats of formation in kJ/mol*

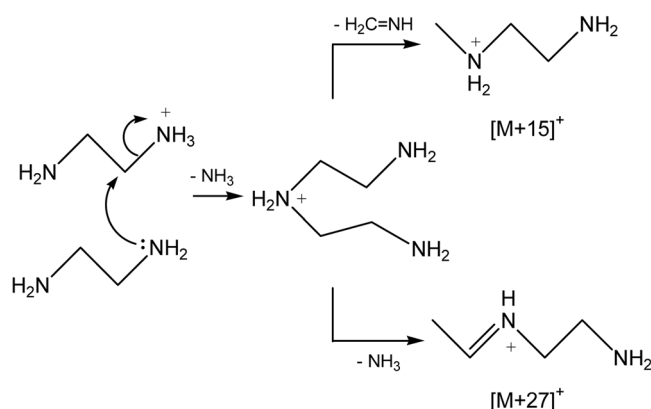
Reaction	ΔH (kJ/mol)
$H_2C=NH_2^+$ (745) + $H_2NCH_2CH_2NH_2$ (-18)	
→ $H_2NCH_2CH_2NH=CH_2^+$ (686) + NH_3 (-46)	-87
→ $H_2NCH_2CH_2NH_3^+$ (570) + $H_2C=NH$ (78)	-79
$H_2C=NH_2^+$ (745) + $H_2NCH_2CH_2OH$ (-202)	
→ $HOCH_2CH_2NH=CH_2^+$ (492) + NH_3 (-46)	-97
→ $H_2NCH_2CH_2O=CH_2^+$ (627) + NH_3 (-46)	38
→ $HOCH_2CH_2NH_3^+$ (378) + $H_2C=NH$ (78)	-87
$H_2C=OH^+$ (703) + $HOCH_2CH_2OH$ (-389)	
→ $HOCH_2CH_2O=CH_2^+$ (409) + H_2O (-242)	-147
→ $HOCH_2CH_2OH_2^+$ (308) + $H_2C=O$ (-109)	-115

*Heats of formation for the neutral molecules were obtained from reference 17.

observed within 1.0 s of the ion trapping time as shown in Figures 2(a), 3(a), and 4(a), respectively. For **EA**, the formations of product ions with a cationic site on oxygen are endothermic while those on nitrogen are exothermic as listed in Table 3. Therefore, we can say that the $[M+13]^+$ ion formed from the reaction of $H_2C=NH_2^+$ with **EA** is $HOCH_2-CH_2NH=CH_2^+$ not $H_2NCH_2CH_2O=CH_2^+$.

Ion-Molecule Reactions between Protonated Molecule and Neutral Molecule. By increasing the ion trapping time, the fragment ions are significantly decreased by the proton transfer reactions and the mass spectra are composed of ions with m/z larger than the molecular ion. Protonated molecule generated by the proton transfer reactions can react with a neutral molecule to generate product ions with m/z larger than the $[M+H]^+$. Ions with m/z larger than the protonated molecule are $[M+15]^+$, $[M+27]^+$, and $[2M+H]^+$ at the ion trapping time of 10.0 s as shown in Figures 2(b), 3(b), and 4(b). The protonated dimer, $[2M+H]^+$, is more abundant than the $[M+15]^+$ and $[M+27]^+$. This implies that the formation of $[2M+H]^+$ is more favorable than those of $[M+15]^+$ and $[M+27]^+$.

The $[M+15]^+$ and $[M+27]^+$ ions were only observed after the ion trapping time which the protonated molecule becomes the most abundant ion. For **DA** and **EA**, the $[M+15]^+$ and $[M+27]^+$ were observed at longer ion trapping time than 1.0 s. For **EG**, the $[M+27]^+$ ion was observed at



Scheme 2. Formation of $[M+15]^+$ and $[M+27]^+$ by ion-molecule reaction.

longer ion trapping time than 100 ms but the $[M+15]^+$ ion was not observed overall ion trapping time. The $[M+15]^+$ and $[M+27]^+$ are formed by the ion-molecule reactions of the protonated molecule with a neutral molecule and loss of neutral molecules such as NH_3 (or H_2O) + $H_2C=NH$ (or $H_2C=O$) and $2NH_3$ (or $2H_2O$), respectively. Mechanisms for the ion-molecule reactions to form $[M+15]^+$ and $[M+27]^+$ of **DA** are shown in Scheme 2. There are two paths for the reactions of protonated **DA** with neutral **DA**. The first one is the formation of $H_2NCH_2CH_2NH_2CH_3^+$, $[M+15]^+$, generated by rearranging and losing NH_3 and $H_2C=NH$. The other one is the formation of $H_2NCH_2CH_2NH=CHCH_3^+$, $[M+27]^+$, generated by rearrangement and loss of two NH_3 .

The formations of $[M+27]^+$ are exothermic while those of $[M+15]^+$ are endothermic as listed in Table 4. The experimental results show that the $[M+27]^+$ are more abundant than the $[M+15]^+$ as shown in Figures 2(b), 3(b), and 4(b).

Table 4. Heats of reaction for the ion-molecule reactions of protonated molecule with neutral molecule. Values in parentheses are heats of formation in kJ/mol*

Reaction	ΔH (kJ/mol)
$H_2NCH_2CH_2NH_3^+$ (570) + $H_2NCH_2CH_2NH_2$ (-18)	
→ $H_2NCH_2CH_2NH_2CH_3^+$ (576) + NH_3 (-46)	56
+ $H_2C=NH$ (78)	
→ $H_2NCH_2CH_2NH=CHCH_3^+$ (570) + $2NH_3$ (-46)	-20
$HOCH_2CH_2NH_3^+$ (378) + $H_2NCH_2CH_2OH$ (-202)	
→ $HOCH_2CH_2NH_2CH_3^+$ (381) + NH_3 (-46)	50
+ $H_2C=O$ (-109)	
→ $HOCH_2CH_2NH=CHCH_3^+$ (430) + NH_3 (-46)	-34
+ H_2O (-242)	
$HOCH_2CH_2OH_2^+$ (308) + $HOCH_2CH_2OH$ (-389)	
→ $HOCH_2CH_2OHCH_3^+$ (321) + H_2O (-242)	51
+ $H_2C=O$ (-109)	
→ $HOCH_2CH_2O=CHCH_3^+$ (355) + $2H_2O$ (-242)	-48

*Heats of formation for the neutral molecules were obtained from reference 17.

Differences in the heats of reaction between $[M+27]^+$ and $[M+15]^+$ are 76, 84, and 99 kJ/mol for **DA**, **EA**, and **EG**, respectively, as listed in Table 4. The $[M+15]^+$ was not observed in the **EG** mass spectrum as shown in Figure 4(b). This may be due to the big difference in the heats of reaction between $[M+27]^+$ and $[M+15]^+$ (99 kJ/mol).

Conclusion

The $[M+H]^+$ was the most abundant ion in mass spectra after the ion trapping times of 30, 50, and 60 ms for ethylenediamine, ethanolamine, and ethylene glycol, respectively. Rate constants for the proton transfer reactions between the fragment ions and neutral molecules were obtained from the temporal variation of the ion abundances. The fastest reactions of proton transfer reactions were the reactions of CH_2N^+ , CHO^+ , and CH_3O^+ for ethylenediamine, ethanolamine, and ethylene glycol, respectively. Product ions with m/z larger than the protonated molecule were $[M+13]^+$, $[M+15]^+$, $[M+27]^+$, and $[2M+H]^+$. The $[M+13]^+$ was formed by the ion-molecule reaction between $\text{H}_2\text{C}=\text{NH}_2^+$ or $\text{H}_2\text{C}=\text{OH}^+$ and neutral molecule, which formed from ion complex such as $[M+\text{H}_2\text{C}=\text{NH}_2]^+$ or $[M+\text{H}_2\text{C}=\text{OH}]^+$ by rearrangement and loss of NH_3 or H_2O . The $[M+15]^+$, $[M+27]^+$, and $[2M+H]^+$ were formed by the ion-molecule reaction between protonated molecule and neutral molecule. The $[M+15]^+$ and $[M+27]^+$ were formed from $[2M+H]^+$ by rearrangement and loss of NH_3 , H_2O , $\text{H}_2\text{C}=\text{NH}$, or $\text{H}_2\text{C}=\text{O}$.

References

1. Raczyńska, E. D.; Maria, P.-C.; Gal, J.-F.; Decouzon, M. *J. Mass Spectrom.* **2000**, *35*, 1222.
2. Chen, X.; Zhong, D.; Liu, D.; Wang, Y.; Han, Y.; Gu, J. *Rapid Commun. Mass Spectrom.* **2003**, *17*, 2459.
3. Paul, G.; Winnik, W.; Hughes, N.; Schweingruber, H.; Heller, R.; Schoen, A. *Rapid Commun. Mass Spectrom.* **2003**, *17*, 561.
4. El-Deen, I. M.; El-Fattah, M. E. *Bull. Kor. Chem. Soc.* **2003**, *24*, 559.
5. Nibbering, N. M. M. *Acc. Chem. Res.* **1990**, *23*, 279.
6. Dearden, D. A.; Liang, Y.; Nicoll, J. B.; Kellersberger, K. A. *J. Mass Spectrom.* **2001**, *36*, 989.
7. Choi, S. S.; So, H.-Y. *Bull. Kor. Chem. Soc.* **2004**, *25*, 1538.
8. Choi, S. S.; So, H.-Y. *Int. J. Mass. Spectrom.* **2005**, *243*, 249.
9. Choi, S. S.; So, H.-Y.; Kim, B.-T. *Bull. Kor. Chem. Soc.* **2005**, *26*, 609.
10. Harrison, A. G.; Keyes, B. G. *J. Am. Chem. Soc.* **1968**, *90*, 5046.
11. Liou, C.-C.; Eichmann, E. S.; Brodbelt, J. S. *Org. Mass Spectrom.* **1992**, *27*, 1098.
12. Ahmed, M. S.; Hudson, C. E.; Giam, C. S.; McAdoo, D. J. *Org. Mass Spectrom.* **1991**, *26*, 1089.
13. Blanc, P. A.; Güllacar, F. O.; Buch, A. *Org. Mass Spectrom.* **1978**, *13*, 135.
14. Burgers, P. C.; Holmes, J. L.; Hop, C. E. C. A.; Postma, R.; Rutink, P. J. A.; Terlouw, J. K. *J. Am. Chem. Soc.* **1987**, *109*, 7315.
15. Fujii, T.; Kitai, T. *Int. J. Mass Spectrom. Ion Processes* **1986**, *71*, 129.
16. Audier, H. E.; Milliet, A.; Perret, C.; Tabet, J. C.; Varenne, P. *Org. Mass Spectrom.* **1978**, *13*, 315.
17. Lias, S. G.; Liebman, J. F.; Levin, R. D. *J. Phys. Chem. Ref. Data* **1984**, *13*, 695.
18. Eichman, E. S.; Brodbelt, J. S. *J. Am. Soc. Mass Spectrom.* **1993**, *4*, 230.
19. Weber, R.; Levsen, K. *Org. Mass Spectrom.* **1980**, *15*, 138.